



Approaching near real-time biosensing: Microfluidic microsphere based biosensor for real-time analyte detection



Noa Cohen ^{a,1}, Pooja Sabhachandani ^{a,1}, Alexander Golberg ^b, Tania Konry ^{a,*}

^a Department of Pharmaceutical Sciences, Northeastern University, 140 The Fenway, Room 441/ 446, 360 Huntington Avenue, Boston, 02115 MA, USA

^b Centre for Engineering in Medicine, Massachusetts General Hospital, Harvard Medical School, Shriners Burns Institute, Boston, MA, USA

ARTICLE INFO

Article history:

Received 25 August 2014

Received in revised form

28 October 2014

Accepted 12 November 2014

Available online 29 November 2014

Keywords:

Microsphere

Real time detection

Lab on a chip

TNF- α

Cytokine

Antibody

ABSTRACT

In this study we describe a simple lab-on-a-chip (LOC) biosensor approach utilizing well mixed microfluidic device and a microsphere-based assay capable of performing near real-time diagnostics of clinically relevant analytes such as cytokines and antibodies. We were able to overcome the adsorption kinetics reaction rate-limiting mechanism, which is diffusion-controlled in standard immunoassays, by introducing the microsphere-based assay into well-mixed yet simple microfluidic device with turbulent flow profiles in the reaction regions. The integrated microsphere-based LOC device performs dynamic detection of the analyte in minimal amount of biological specimen by continuously sampling micro-liter volumes of sample per minute to detect dynamic changes in target analyte concentration. Furthermore we developed a mathematical model for the well-mixed reaction to describe the near real time detection mechanism observed in the developed LOC method. To demonstrate the specificity and sensitivity of the developed real time monitoring LOC approach, we applied the device for clinically relevant analytes: Tumor Necrosis Factor (TNF)- α cytokine and its clinically used inhibitor, anti-TNF- α antibody. Based on the reported results herein, the developed LOC device provides continuous sensitive and specific near real-time monitoring method for analytes such as cytokines and antibodies, reduces reagent volumes by nearly three orders of magnitude as well as eliminates the washing steps required by standard immunoassays.

© 2014 Elsevier B.V. All rights reserved.

1. Introduction

Rapid, sensitive and quantitative detection methods of disease markers are necessary for timely and effective diagnosis and therapy (Martinez et al., 2008). A major challenge in the detection of soluble molecules such as cytokines, protein antigens and antibodies is the ability to monitor time-varying or dynamic concentrations in real-time. Currently there are no online monitoring approaches available for continuous analyte immunoassays and pharmacokinetic characterization of biomolecules in real-time. At present, state-of-the-art analyte detection techniques include immunoassays such as enzyme-linked immunosorbent assays (ELISA) and Luminex assays, which are based on specific recognition of clinical antigens by the respective antibodies (Reichert, 2001; Djoba Siawaya et al., 2008). These diagnostic methods are performed on samples obtained at pre-defined times and are therefore laborious

and time-intensive procedures. Additionally, these methods are impractical for real-time monitoring since they cannot be performed rapidly enough to assess dynamic fluctuation of analyte concentration *in vivo*. This limits their utility in clinical settings where it is of critical importance to generate real-time profile of analytes such as cytokines or administered drugs *in vivo* (Crowther, 2001; Mannerstedt et al., 2010; Mao et al., 2009; Wild, 2001).

In non-mixed solutions, like immunosorbent assays (ELISA), the binding reaction rates for reagents with low binding equilibrium constant, such as high affinity antibody-antigen interaction, depend on diffusion (Porstmann and Kiessig, 1992). Further increase of reaction surface or decrease of reaction volumes will not decrease the reaction time (Crowther, 2001). Therefore most, if not all, non-mixing immunoassay systems require incubation of 1–2 h for analyte detection (Kusnezow et al., 2006; Ruslinga et al., 2010). Several developments in microfluidic based immunosorbent assay have been reported within the past ten years to address the circumventing problems associated with conventional immunoassays (Chen et al., 2011; Hou and Herr, 2010; Lee et al., 2009; Ng et al., 2010, 2012; Nie et al., 2014; Rissin et al., 2010; Thaitrong et al., 2013; Bange et al., 2005). In the microfluidic

* Corresponding author.

E-mail addresses: konry.tania@gmail.com, t.konry@neu.edu (T. Konry).

¹ Equal contribution.

immunoassay format increased surface area to volume ratios speed up the antibody–antigen reactions while the smaller dimensions reduce the consumption of expensive reagents and precious samples (Kai et al., 2012; Thaitrong et al., 2013). Never the less most of these methods still require incubation and are unable to measure dynamic changes in the analyte concentration in real time (Hu et al., 2007; Singhal et al., 2010).

Most of proposed optical micro-devices today are based on patterning lines of immobilized capture antibodies (Abs) in the micro-channels of the device and exposing these lines orthogonally to solutions of analytes (Hu et al., 2007; Singhal et al., 2010; Wolf et al., 2004). Then specifically captured analytes are detected with fluorescently labeled detection Abs creating a micromosaic of fluorescent zones, which reveals the binding events in a single imaging step. At this small scale, fluids exhibit laminar flow, i.e. fluidic streams that flow parallel to each other, and mixing occurs only by diffusion. Although diffusion distances in microchannels are significantly reduced in comparison to conventional microtiter well plate formats, analytes are still transport-limited in microchannels at low sample concentrations (Parsa et al., 2008). Thus both analyte capture and the fluorescently labeled antibody binding to the captured analyte still require an incubation step.

One of the strategies to improve the analyte capture and detection of Ab binding is to integrate mixing elements in the microfluidic device (Hu et al., 2007). Herein we were able to overcome the adsorption kinetics limitation controlled by diffusion rates by introducing the microsphere-based assay into well-mixed yet simple microfluidic device with turbulent flow profiles in the reaction region. In this microfluidic device the micro-liter volumes of sample as well as microsphere-based assay reagents are continuously replenished in the device to perform continuous detection of the analyte in minimal amount of biological specimen. Integrating microsphere-based immunoassays with the developed herein microfluidics has major advantage over flat-surface assays such as ELISA (Crowther, 2001; Mannerstedt et al., 2010); microspheres have larger surface area (Nie et al., 2014), so the interaction between microspheres and target molecules in the well-mixed flow based format are practically comparable with solution-phase kinetics. Furthermore, due to the fast reaction kinetics, this lab-on-a-chip (LOC) approach is capable of performing near real-time detection of clinically relevant analytes such as cytokines, proteins, antibodies and drugs.

We applied the above-described LOC device for measuring Tumor Necrosis Factor (TNF)- α cytokine and TNF- α inhibitor, anti-TNF- α antibody in a sample. TNF α is a member of a group of cytokines that stimulates the acute phase reaction in systemic inflammation (Balkwill, 2006; Bradley, 2008; Yeh et al., 1997; Feldman and Maini, 2003). The TNF- α signaling pathway has been attributed a major role in pathological processes of diseases such as chronic inflammation, (Bradley, 2008; Yeh et al., 1997) autoimmune disorders (Feldman and Maini, 2003), and cancer (Balkwill, 2006). The TNF- α inhibition can be achieved with therapeutic antibodies such as Infliximab (Remicade), Adalimumab (Humira), Certolizumab pegol (Cimzia), and Golimumab (Simponi) (Brustolim et al., 2006; David and Essayan, 2001; Marques et al., 1999; Scallon et al., 2002). Thus, the ability to monitor dynamic changes in TNF- α concentration and to correlate this profile to the inflammation level in patients after inhibitory treatment as well as pharmacokinetic studies of TNF- α inhibitors such as anti-TNF- α agents is of great interest (Feuerstein et al., 1994; Locksley et al., 2001).

The sensitivity and specificity of the developed LOC method were tested and compared to the standard immunoassays available commercially. The developed LOC method allowed us to reduce reagent volumes by nearly three orders of magnitude, eliminate the washing steps required by standard immunoassays, and

enhance detection reaction rates to accomplish near real-time monitoring of clinically relevant targets. In particular, we were able to determine that the time to obtain a specific conjugation/coverage on the microsphere surface in well-mixed microfluidic LOC is achieved in seconds in the flow through incubation channel compared to 1–2 h in the non-well mixed solutions, thus allowing near real-time detection in the developed LOC. Furthermore the developed simple LOC platform can be applied for real time point of care diagnostics of inflammation, infectious diseases and other diseases where the detection is based on antibody–antigen interactions for specific detection of the disease clinical markers.

2. Materials and methods

2.1. Microfluidic device fabrication

The Polydimethylsiloxane (PDMS) microfluidic device was fabricated using well-established soft lithography method. Negative photo resist SU-8 2100 (MicroChem, Newton, MA) was spin coated on Silicon wafers to a thickness of 150 μm , and patterned by exposure to UV light through a transparency photomask (CAD/Art Services, USA). PDMS (Sylgard 184, Dow Corning, MI) was mixed with the crosslinker (Sylgard 184 curing agent) in a ratio of 10:1, poured onto the photoresist patterns, degassed thoroughly and cured for 12 h at 65 $^{\circ}\text{C}$. Next, the PDMS was peeled off the wafer and placed in oxygen-plasma chamber in order to bond with the glass slide. The device consists of three inlets and two serpentine mixing regions. Tygon Micro Bore PVC Tubing 0.010" ID, 0.030" OD, 0.010" Wall (Small Parts Inc., FL, USA) was connected to the channels and to 1 mL syringes. Syringe pumps (Harvard Apparatus, USA) were used to maintain a flow rate of 5 $\mu\text{L}/\text{min}$ through the device.

2.2. Microsphere sensor preparation

For anti-TNF- α antibody detection, biotinylated human TNF- α protein (ACRO Biosystem, Cat. no. TNA-H8211) was conjugated to streptavidin-coated polystyrene microsphere of diameter 6.8 μm (0.5% w/v, Spherotech Inc.). A 50 μL aliquot of the microsphere solution was washed with 1 \times Phosphate Buffered Saline (PBS) (Sigma, USA) and diluted to a final concentration of 0.25 mg/ml in PBS with 0.005% (v/v) Tween 20 (Sigma, USA). 40 μg of human TNF- α protein was added per mg of microspheres, and the mixture was shaken at room temperature (RT) for 120 min. Unbound active sites were blocked with BlockAid (B-10710, Invitrogen) for 1 h. Finally, the microspheres were washed with PBS and stored at 4 $^{\circ}\text{C}$ in 0.5% (w/v) Bovine Serum Albumin (BSA) (Sigma, USA) in PBS. The analyte for dose response experiments, mouse monoclonal antibody to human TNF- α (Sino Biological Inc., USA, Cat. no. 10602-MM01), was diluted to the following concentrations in 1 \times PBS: 100, 250, 500, 750 and 1000 ng/mL. The detection antibody, goat anti-mouse IgG-FITC (Sigma, USA, Cat. no. F0257) was mixed with Pierce Immunostain Enhancer (Thermo Scientific, USA) to obtain a final concentration of 13.8 $\mu\text{g}/\text{mL}$.

For TNF- α detection, a 200 μL (1 mg) aliquot of Protein G polystyrene microspheres (0.5% w/v, Spherotech Inc.) was washed with 800 μL of PBS and centrifuged. 200 μL of rabbit anti-human TNF- α (Thermo Scientific, USA, Cat. no. P300A) was diluted with 100 μL of 0.5% BSA/PBS (0.22 mg) and was added to the microspheres. The mixture was shaken at RT for 120 min. Unbound active sites were blocked with 1 mL of BlockAid for 1 h. Finally, the microspheres were washed with PBS and stored at 4 $^{\circ}\text{C}$ in 0.5% (w/v) BSA/PBS. For dose response experiments, *Escherichia coli*-derived recombinant rat TNF- α (R&D Systems, USA, Cat. no. AGM0213082) was diluted to the following concentrations in 1 \times

PBS: 0.02, 1, 50, 100 and 1000 ng/mL. The hamster anti-TNF- α FITC (eBioscience, USA, Cat. no. 11-7423) was diluted in Pierce Immunostain Enhancer to a final concentration of 13.8 $\mu\text{g}/\text{mL}$.

2.3. Data and image analysis

The fluorescent microspheres for detection of the analytes were assessed and recorded using Zeiss Axio Observer.Z1 Microscope (Zeiss, Germany). Images were taken with Hamamatsu digital camera C10600 Orca-R2 using the ZEN pro 2012 software (blue edition). ImageJ software was used for image analysis and processing. The microsphere of interest was selected, outlined and the area, integrated density and mean gray value were measured. The background fluorescence was selected as a random circular region in the microfluidic channels, near the fluorescent microsphere. At least thirty fluorescent microspheres were analyzed for each sample. Microsoft Office Excel 2010 and Origin were applied for statistical analysis analyses.

2.4. Binding kinetics model

In the following section we describe the supporting equations for non-well mixed solutions that were amended in the developed theoretic model on reaction kinetics in the well-mixed LOC describe in the results section. The general conservation equation that described the reaction in the fluid bulk appears in (Gervais and Jensen, 2006) as

$$\partial C/\partial t + \nabla(-D\nabla C + vC) = R_v \quad (1)$$

where C is the bulk concentration of an analyte, D is the bulk analyte diffusivity, and v is the fully developed velocity profile of the analyte in the bulk. R_v is the analyte creation volumetric rate. The initial condition for the analyte concentration in the bulk is as follows:

$$C(t=0) = C_0 \quad (2)$$

The conservation equation for the detecting surface that includes the surface diffusion and the reaction rate for the formation

of the absorbed analyte appears in Eq. (3):

$$\partial C_s/\partial t + \nabla(-D_s\nabla C_s) = k_{on}C_{(n=0)}(C_{s0} - C_s) - k_{off}C_s \quad (3)$$

where C_s is the surface concentration of an analyte, D_s is the analyte surface diffusivity $C_{n=0}$ is the concentration of bulk analyte near the reactive bead wall, C_{s0} is the total number of the binding sites, k_{on} is the association rate constant and k_{off} is the dissociation rate constant of the binding reaction. The initial condition for Eq. (3) is the concentration of the absorbed species on the detecting surface at the beginning of the process is:

$$C_s(t=0) = 0 \quad (4)$$

Eqs. (1) and (3) are coupled through the flux balance boundary condition on the reacting surface as follows:

$$n(-D\nabla C + vC) = -k_{on}C_{(n=0)}(C_{s0} - C_s) + k_{off}C_s \quad (5)$$

where n is the surface vector. The additional boundary condition on non-reactant surfaces is insulation:

$$n(-D_s\nabla C_s) = 0 \quad (6)$$

Previously, Kankare and Vinokurov (1999) developed the mathematical model that describes reaction kinetics in standard, non-mixed immunosorbent reactions, where absorption occurs on spherical surfaces. To solve the general conservation equation for the reaction in the fluid bulk (Eqs. (2)–(8)), the authors used the following assumptions: (1) reaction takes place in the non-agitating solution; therefore, $v=0$; (2) no reagents are formed in the bulk; therefore, $R_v=0$; (3) no surface diffusivity of the absorbed analyte; thus, $D_s=0$; and (4) constant diffusivity of the analyte in the liquid ($D=\text{const.}$) (Kankare and Vinokurov, 1999). We followed this model to calculate the reaction time (t_h) on microsphere in the non-agitating solution.

According to Kankare and Vinokurov (1999) Eqs. (7)–(13) describe the analyte absorption on the spherical microsphere in the non-mixed immunosorbent reaction.

$$\partial C/\partial t - D(d^2/dn^2) - 2D/(n+R)\partial C/\partial n = 0 \quad (7)$$

where R is the detection microsphere radius.

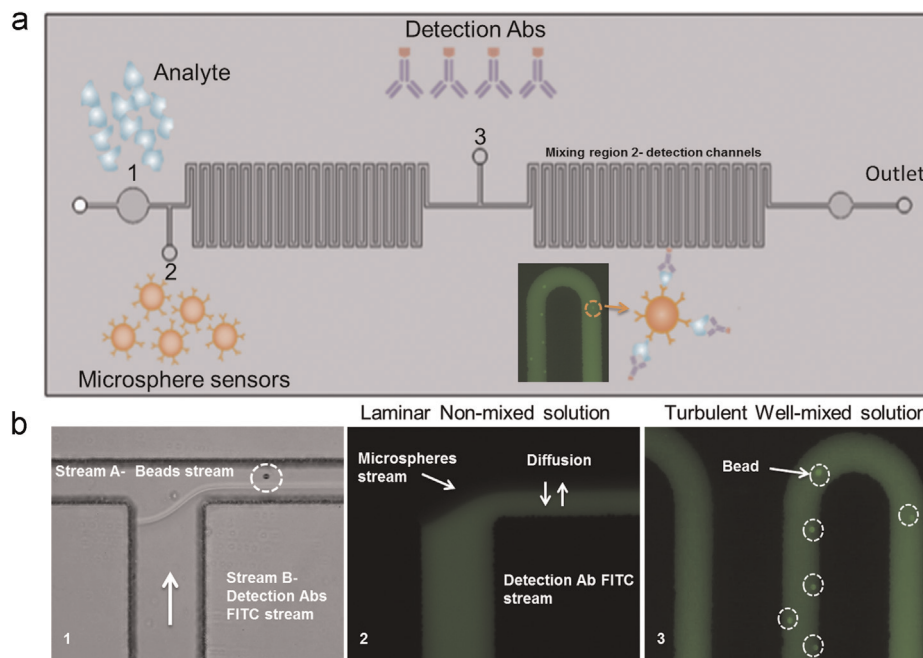


Fig. 1. Flow dynamics in the designed microfluidic device. (a) Schematic illustration of the microfluidic microsphere based LOC device. (b) Microscope images of the flow: 1. Phase image of Inlet 3. 2. Fluorescent image of inlet 3. 3. Fluorescent image of detection channels with sandwich complex formation on microspheres.

The initial condition for the analyte concentration in the bulk is:

$$C(t = 0) = C_0 \quad (8)$$

The surface reaction equation is as follows:

$$\partial C_s / \partial t = k_{on} C_{(n=R)} (C_{s0} - C_s) - k_{off} C_s \quad (9)$$

with initial condition:

$$C_s(t = 0) = 0 \quad (10)$$

The coupling boundary condition is as follows:

$$n(-D\nabla C) = -k_{on} C_{(n=0)} (C_{s0} - C_s) + k_{off} C_s \quad (11)$$

The numerical solution of this set of equations shows that the time to achieve full surface coverage of the analyte on the microsphere surface (equilibrium) in non-mixed solution is infinity. Therefore, an important outcome from this numerical solution for non-mixed solutions is the approximation for the time needed for the reaction to achieve a certain deviation from the equilibrium coverage (h) on the spherical microsphere:

$$\lim_{k_{on} \rightarrow \infty} t_h \approx - (Rk_{on}C_{s0}) / (k_{off}D(1 + k_{on}/k_{off}C)0^2) \ln h \quad (12)$$

where h is the deviation from the equilibrium coverage:

$$h = (C_{s0} - C_s) / C_{s0} \quad (13)$$

The solution of these equations implies that in microsphere-based immunosorbent assay, in the non-mixed solutions, the binding reaction rates for reagents with low binding equilibrium constant depend on diffusion, and further increase of the reaction surface or the decrease of reaction volumes will not decrease the reaction time (Kusnezow et al., 2006).

3. Results and discussion

3.1. Flow dynamics in the designed microfluidic device

Fig. 1a schematically illustrates the developed flow-through LOC device. The device consists of three inlets and two mixing regions. The inlets are connected with syringe pumps that are operated individually to obtain desired flow rates for the detection of microspheres downstream. First, a solution containing the analyte molecules is introduced into inlet 1 and is mixed with a suspension of functionalized microspheres that are introduced via inlet 2 to capture the target analyte in the mixing region 1 (Fig. 1a). The specific interaction that occurs between the conjugated microspheres and the target analyte in the well-mixed serpentine channel leads to the analyte recognition and capture. A detection (reporter) antibody against the analyte, conjugated with a specific fluorophore, is then introduced to the flow stream (inlet 3) just before the serpentine mixing region 2. The sandwich complex formation, composed of microsphere sensor–analyte–reporter antibody, results in high levels of intensity fluorescent signal on the microsphere that is easily distinguishable from the background intensity. The fluorescence from the reporter antibodies is detected downstream to the second serpentine mixing region (Fig. 1b).

The flow profile in the developed microfluidic device consists of laminar flow and turbulent profiles in distinct regions of the device (Fig. 1b). Laminar flow in the developed LOC occurs when a fluid streams A and B flow in parallel layers, with no disruption between the layers (Fig. 1b(1,2)). As observed in Fig. 1b(1), the microsphere in stream A moves in straight lines parallel to the channel wall. In fluid dynamics, laminar flow is characterized by

high momentum diffusion and low momentum convection (Batchelor, 2000; Bayraktar and Pidugu, 2006; Beebe et al., 2002). Thus, in this region the microsphere adsorption kinetics are controlled by diffusion rates between upper stream A to the lower stream B and vice versa and thus will follow a non-mixed immunoassay reaction such as described in ELISA (Kankare and Vinokurov, 1999). The fluid flow is altered markedly when it travels over an abrupt serpentine feature just as wind going over a mountain ridgeline (Fig. 1b(3)) (Sharp and Adrian 2004). The narrowing U shape serpentine geometry causes a change in the flow profile from diffusion-controlled laminar profile to turbulent well-mixed solution in the incubation channels. Fig. 1b(3) shows the instantaneous position of the microspheres in the carrier fluid in the well-mixed incubation channel. It is apparent that the particles are distributed in a highly non-homogeneous manner in the incubation channel, forming clusters and voids as well as spontaneously segregating different regions of the flow in the channel. Thus, individual microspheres follow paths that are independent and largely random in this turbulent fluid stream. Next, the detection antibody, FITC-labeled anti-mouse IgG, was introduced into inlet 3. The fluorescent signal on the microsphere sensor, generated by the conjugation of the captured anti-TNF- α antibody with the fluorescently labeled detection antibody is demonstrated in Fig. 1b(3). The high surface-to-volume ratio of the microsphere (Lim and Zhang, 2007), as well as the turbulent mixing (Sharp and Adrian 2004) generated within the serpentine structure of microfluidic device, reduces the incubation time for the detection to seconds, as will be demonstrated below, thereby enabling continuous flow-through detection.

3.2. LOC biosensor detection

3.2.1. Anti-TNF- α antibody immunoassay

To demonstrate the real-time detection capabilities of our LOC device we first focused on detecting anti-TNF- α antibody. Fig. 2a describes the microsphere-based assay that was introduced into microfluidic format for anti-TNF- α detection. Avidinylated microspheres were conjugated off-chip to biotinylated human TNF- α protein via avidin–biotin bridge (Konry et al., 2009; Diamdandis and Christopoulos, 1991) as described in the Experimental Section. Next, the generated anti-TNF- α microsphere-based sensors were introduced into the microfluidic device via inlet 2 while the analyte, mouse monoclonal anti-human TNF- α antibody, was introduced via inlet 1 (Fig. 3a(1)). The interaction of the two

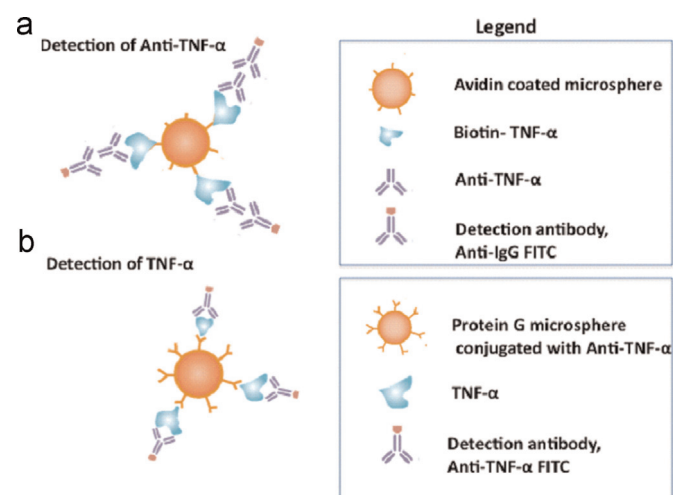


Fig. 2. Schematic illustration of microsphere based sensors. (a) Microsphere based detection of anti-TNF- α antibodies. (b) Microsphere based detection of TNF- α cytokine.

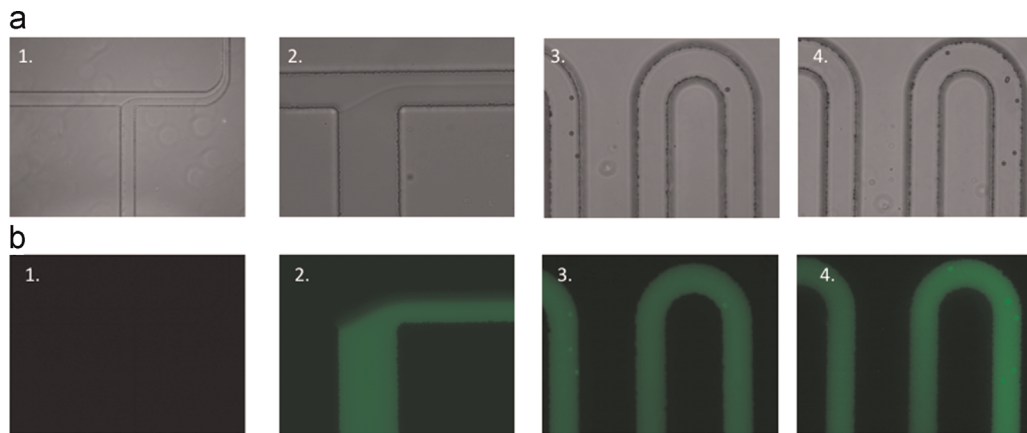


Fig. 3. (a) 1. Phase image of: 1. Intersection of inlet 1 (analyte) and inlet 2 (microsphere sensors). 2. Intersection of mixing region 1 and inlet 3 (detection antibody). 3. Detection region of the anti-TNF- α antibodies in the incubation channel. 4. Detection region of TNF- α in the incubation channel. (b) Corresponding fluorescent images of panel a.

components resulted in the capture of anti-TNF- α antibodies by microsphere-based sensors in the first incubation channel of the device (Fig. 1a). Next, the detection antibody, FITC-labeled anti-mouse IgG, was introduced into inlet 3 (Figs. 1a and 3a). The fluorescent signal on the microsphere sensor, generated by the conjugation of the captured anti-TNF- α antibody with the fluorescently labeled detection antibody is demonstrated in Fig. 3b (3).

The standard curve for the anti-TNF- α antibody immunoassay was obtained by collecting data from thirty microspheres for each concentration point ranging from 100 to 1000 ng/mL in the device. Fig. 4a shows a typical behavior for the standard calibration curve with an exponential growth, as seen from the curve fit, which results in a linear range shown in Fig. 4b. The curve fit in Fig. 4b was carried out using an equation of the form $y = A + B(x)$, where x is the anti-TNF- α antibody concentration and y is the corresponding fluorescent response signal obtained. The standard curve was most useful for quantization of concentrations from 100 ng/ml and higher, showing in this range an acceptable square correlation coefficient, R^2 , of 0.94 and a satisfactory sensitivity of 3.67 relative fluorescence units (RFU) (determined within the linear concentration range of the biosensor as the slope, B , of the calibration curve). At higher concentrations, the curve levels off with a response saturation observed from concentration 750 ng/ml and above. The detection limit of the immunosensor, was defined as the amount (or concentration) of the analyte that gives a response, that is significantly different (three standard deviations from the background analysis that is itself obtained from negative control, a sample without analyte). The background signal recorded for the blank (in absence of the analyte, Table 1a, experiment 3) and its calculated standard deviation allowed us to reach a limit of quantization for a concentration of anti-TNF- α as low as 100 ng/mL that was recorded in the incubation channel after 22.7 s in flow. Thus the developed microsphere based LOC device demonstrates higher detection sensitivity for anti-TNF- α antibodies than that recorded previously in well-established immunoassays such as ELISA, where the detection limit was reported to be 0.5–1 $\mu\text{g/mL}$ (Sino Biological Inc., Cat. no. 10602-MM01). To validate the specificity of the developed LOC assay we conducted a set of experiments described in Table 1a. The results in Table 1a show that the responses from experiments 2 and 3 (in absence of capture molecule and analyte) are all relatively negligible.

3.2.2. TNF- α cytokine immunoassay

Our next goal was the adaptation of this LOC device for TNF- α cytokine detection in real-time. Fig. 2(b) describes the microsphere-based assay using TNF- α as a model cytokine. In this

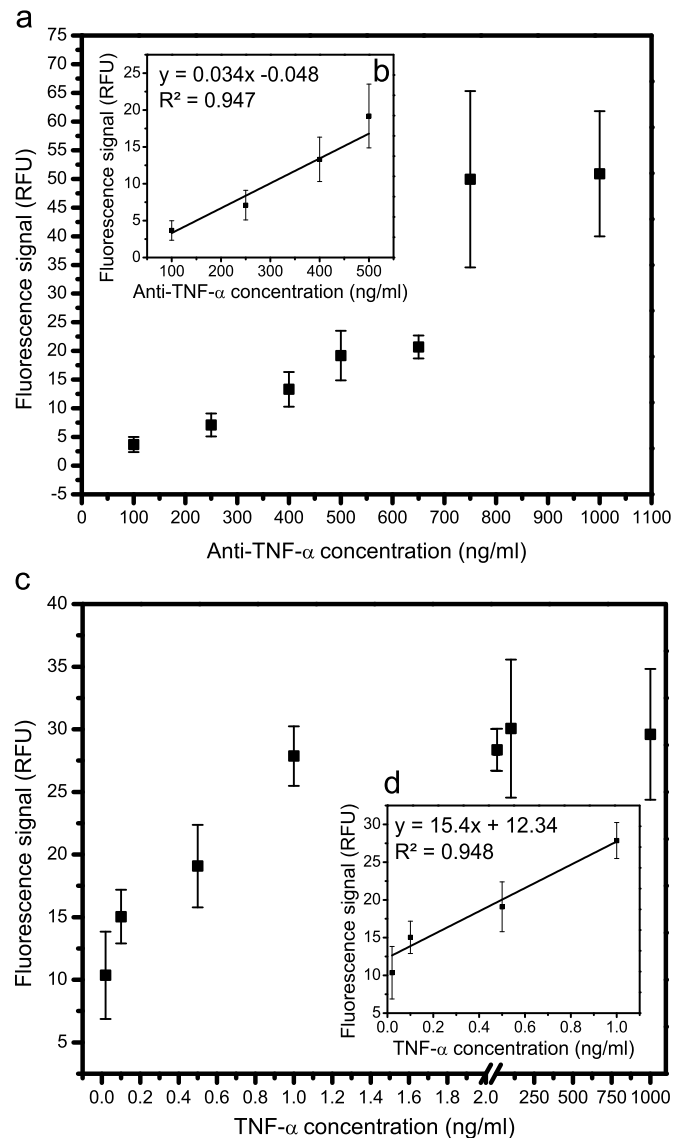


Fig. 4. Dose response graphs for (a) anti-TNF- α antibody. (b) Linear concentration range of the biosensor for anti-TNF- α antibody. (c) TNF- α cytokine. (d) Linear concentration range of the biosensor for TNF- α cytokine.

Table 1

Experiments carried out in order to determine the possible influence of nonspecific effects on the obtained response. The (+) and (–) signs indicate the steps accomplished or avoided respectively for each experiment. The response was recorded in all the experiments for (a) anti-TNF-α antibodies and (b) TNF-α cytokine. Responses of experiments 2 and 3 were normalized to experiment 1.

EXP.	Avidin Microsphere	Biotinylated human TNF-α	Mouse-Anti to Human TNF-α	Anti-Mouse IgG-FITC	Normalized response
(a)					
1.	+	+	+	+	1
2.	+	–	+	+	0.03
3.	+	+	–	+	0.16
EXP.	Protein G microsphere	Anti- TNF-α	TNF-α	Anti- TNF-α FITC	Normalized response
(b)					
1.	+	+	+	+	1
2.	+	–	+	+	0.14
3.	+	+	–	+	0.18

system, protein-G microspheres were conjugated off-chip to anti-TNF-α antibodies as described in Section 2. Next, the generated microsphere-based sensors were introduced into the microfluidic device via inlet 2 while the analyte, TNF-α, was introduced via inlet 1 (Fig. 1a). The interaction of the two components resulted in the capture of TNF-α by microsphere-based sensors in the first incubation channel of the device. Next, the detection antibody, FITC-labeled anti-rat TNF-α antibody, was introduced into inlet 3 (Fig. 1a). The fluorescent signal on the microsphere sensor, generated by the conjugation of the captured TNF-α with the fluorescently labeled detection antibody is demonstrated in Fig. 3(b(4)).

The standard curve for the TNF-α immunoassay was obtained by collecting data from thirty microspheres for each concentration point ranging from 0.02 to 1000 ng/mL in the device. Fig. 4c shows a typical behavior for the standard calibration curve with an exponential growth, as seen from the curve fit, which results in a linear range shown in Fig. 4d. The curve fit was carried out using an equation of the form $y = A + B(x)$, where x is the TNF-α antibody concentration and y is the corresponding fluorescent response signal obtained. The standard curve was most useful for quantization of concentrations from 0.02 ng/ml and higher, showing in this range an acceptable square correlation coefficient, R^2 , 0.95 and a satisfactory sensitivity of 10.36 RFU (determined within the linear concentration range of the biosensor as the slope, B , of the calibration curve). At higher concentrations, the curve levels off with a response saturation observed from concentration 100 ng/mL and above. The detection limit of the immunosensor, defined as the amount (or concentration) of the analyte that gives a response, that is significantly different (three standard deviations from the background analysis that is itself obtained from negative control, a sample without analyte). The background signal recorded for the blank (in absence of the analyte, Table 1b, experiment 3) and its calculated standard deviation allowed us to reach a limit of quantization for a concentration of TNF-α as low as 0.02 ng/ml that was recorded in the incubation channel after 22.4 s in flow. This is to similar sensitivity previously reported by standard ELISA method (R&D systems, Cat. no. 510-RT-010, sensitivity 0.05 of ng/mL) and commercially available luminex assay (Human TNF-α Singleplex Bead Kit, Invitrogen, Cat. no. LHC3011, sensitivity 0.01 ng/ml). To validate the specificity of the developed LOC assay we conducted a set of experiments described in Table 1b. The results in Table 1b show that the responses from

experiments 2 and 3 (in absence of capture molecule and analyte) are all relatively negligible.

3.3. Mathematical model for well-mixed LOC device

Mathematical model developed for well-mixed LOC device. In non-mixed solutions in microsphere-based immunosorbent assay and ELISA, the binding reaction rates for reagents with low binding equilibrium constant, such as high affinity antibody–antigen interaction, depend on diffusion (Porstmann and Kiessig, 1992). Further increase of reaction surface or decrease of reaction volumes will not decrease the reaction time. Therefore most, if not all, non-mixing immunoassay systems are incubated for 1–2 h (Kusnezow et al., 2006; Ruslinga et al., 2010). Integrating microsphere-based immunoassays with microfluidic LOC has one major advantage over flat-surface assays such as ELISA (Crowther, 2001; Mannerstedt et al., 2010); microspheres have larger surface area, so the interaction between microspheres and target molecules in flow based format is practically comparable with solution-phase kinetics. This integrated format allowed us to observe the changes in levels of analytes in near real time since all reagents are continuously replenished in the device.

To support our finding of real-time detection, we developed a mathematical model for in-flow well-mixed immunoassay reaction on a microsphere surface. In our experimental setup, the microspheres move within the well-mixed solution in incubation channels (Fig. 1(b)). The fast mixing profile of the reaction reagents in the serpentine channels implies that the adsorption reaction on the detecting microspheres is different from classical non-mixed bulk immunosorbent assays like ELISA. The equations describing detection reaction inside the mixing LOC channel are as follows:

$$A + B \xrightleftharpoons[k_{off}]{k_{on}} AB \quad K_D = \frac{K_{off}}{K_{on}} = \frac{[A][B]}{[AB]} \quad (14)$$

$$\partial C_s / \partial t = k_{on} C_d (C_{s0} - C_s) + k_{off} C_s \quad (15)$$

With the initial condition

$$C_s(t = 0) = 0 \quad (16)$$

where A is the analyte, B is the detection antibody, AB is the analyte–detection antibody complex, C_s is the surface concentration of an analyte on the microsphere, C_d is the analyte concentration in the bulk volume, C_{s0} is the maximum concentration of the analyte on the microsphere, predefined by the total number of the binding sites, k_{on} is the association rate constant and k_{off} is the dissociation rate constant of the binding reaction, and k_d is the dissociation constant and t is the reaction time.

The complete solution for concentration of the molecule of interest on the microsphere appears in Eq. (17):

$$C_s = -k_{on} C_d C_{s0} / (k_{on} C + dk_{off}) \exp(- (k_{on} C + dk_{off}) t) + k_{on} C_d C_{s0} / (k_{on} C + dk_{off}) \quad (17)$$

Thus the time t_h for reaction in the well-mixed channels for a deviation h from the equilibrium coverage (Eq. 13) is:

$$t_h = - (k_{on} C + dk_{off})^{-1} \ln(h(1 + k_{off}/k_{on} C_d) - k_{off}/k_{on} C_d) \quad (18)$$

and specifically, for analyte/antigen–antibody reactions with small dissociation constant thus with large k_{on} (Song et al., 2008):

$$\lim_{k_{on} \rightarrow \infty} t_h \approx 0 \quad (19)$$

Thus, in well-mixed reactors, the conjugation/coverage (h) on the moving microsphere surface can be achieved almost instantly in the ideal systems with very low dissociation constants. These

fundamental differences in the reaction kinetics limiting step makes the developed mixing channel technology an ideal system for miniaturized immunosorbent reactions as it overcomes the major constraint of the rapid detection-diffusion.

4. Conclusion

In summary, the developed LOC biosensor allowed us to reduce reagent volumes by nearly three orders of magnitude, eliminate the washing steps required by standard immunoassays, as well as enhance detection reaction rates to accomplish near real-time monitoring of clinically relevant targets. In particular, we were able to determine that the time to obtain a specific conjugation/coverage h on the microsphere surface in well mixed microfluidic LOC is achieved in seconds in the flow through incubation channel compared to 1–2 h in the non-mixed solutions, thus allowing near real-time detection in the developed LOC. Furthermore the specificity and sensitivity of the developed LOC device is comparable to the standard immunoassay for clinically relevant analytes, TNF- α cytokine and anti-TNF- α antibody.

References

- Balkwill, F., 2006. *Cancer Metastasis Rev.* 25, 409–416.
- Bange, A., Halsall, H.B., Heineman, W.R., 2005. *Biosens. Bioelectron.* 20, 2488–2503.
- Batchelor, G., 2000. *Introduction to Fluid Mechanics*. Cambridge University Press, UK reprinted, Cambridge.
- Bayraktar, T., Pidugu, S.B., 2006. *Int. J. Heat Mass Transf.* 49, 815–824.
- Beebe, D.J., Mensing, G.A., Walker, G.M., 2002. *Annu. Rev. Biomed. Eng.* 4, 261–286.
- Bradley, J.R., 2008. *J. Pathol.* 214, 149–160.
- Brustolim, D., Ribeiro-dos-Santos, R., Kast, R.E., Altschuler, E.L., Soares, M.B., 2006. *Int. Immunopharmacol.* 6, 903–907.
- Chen, C.H., Sarkar, A., Song, Y.A., Miller, M.A., Kim, S.J., Griffith, L.G., Lauffenburger, D.A., Han, J., 2011. *J. Am. Chem. Soc.* 133, 10368–10371.
- Crowther, J.R., 2001. *The ELISA Guidebook*. Humana Press Inc., New Jersey.
- David, M., Essayan, 2001. *J. Allergy Clin. Immunol.* 108, 671–680.
- Diamandis, E.P., Christopoulos, T.K., 1991. *Clin. Chem.* 37, 625–636.
- Djoba Siawaya, J.F., Roberts, T., Babb, C., Black, G., Golakai, H.J., et al., 2008. *PLoS ONE* 3, e2535.
- Feldman, M., Maini, R.N., 2003. *Nat. Med.* 9, 1245–1250.
- Feuerstein, G.Z., Liu, T., Barone, F.C., 1994. *Cerebrovasc. Brain Metab. Rev.* 6, 341–360.
- Gervais, T., Jensen, K.F., 2006. *Chem. Eng. Sci.* 61, 1102–1121.
- Hou, C., Herr, A.E., 2010. *Anal. Chem.* 82, 3343–3351.
- Hu, G., Gao, Y., Li, D., 2007. *Biosens. Bioelectron.* 22, 1403–1409.
- Kai, J., Puntambekar, A., Santiago, N., Lee, S.H., Sehy, D.W., Moore, V., Hana, J., Ahnab, C.H., 2012. *Lab Chip* 12, 4257–4262.
- Kankare, J., Vinokurov, I.A., 1999. *Langmuir* 15, 5591–5599.
- Konry, T., Hayman, R.B., Walt, D.R., 2009. *Anal. Chem.* 81, 5777–5782.
- Kusnezow, W., Syagailo, Y.V., Ruffer, S., Baudenstiel, N., Gauer, C., Hoheisel, J.D., Wild, D., Goychuk, I., 2006. *Mol. Cell Proteomics* 5, 1681.
- Lee, J.H., Cosgrove, B.D., Lauffenburger, D.A., Han, J.J., 2009. *Am. Chem. Soc.* 131, 10340–10341.
- Lim, C.T., Zhang, Y., 2007. *Biosens. Bioelectron.* 22, 1197–1204.
- Locksley, R.M., Killeen, N., Lenardo, M.J., 2001. *Cell* 104, 487–501.
- Mannerstedt, K., Jansson, A.M., Weadge, J., Hindsgaul, O., 2010. *Angew. Chem. Int. Ed.* 49, 8173.
- Mao, C., Liu, A., Cao, B., 2009. *Angew. Chem. Int. Ed.* 48, 6790.
- Marques, L.J., Zheng, L., Poulakis, N., Guzman, J., Costabel, U., 1999. *Am. J. Respir. Crit. Care Med.* 159, 508–511.
- Martinez, A.W., Phillips, S.T., Carrilho, E., Thomas III, S.W., Sindi, H., Whitesides, G.M., 2008. *Anal. Chem.* 80, 3699–3707.
- Ng, A.H., Choi, K., Luoma, R.P., Robinson, J.M., Wheeler, A.R., 2012. *Anal. Chem.* 84, 8805–8812.
- Ng, A.H.C., Uddayasankar, U., Wheeler, A.R., 2010. *Anal. Bioanal. Chem.* 397, 991–1007.
- Nie, S., Henley, W.H., Miller, S.E., Zhang, H., Mayer, K.M., Dennis, P.J., Oblath, E.A., Alarie, J.P., Wu, Y., Oppenheim, F.G., Little, F.F., Uluer, A.Z., Wang, P., Ramsey, J.M., Walt, D.R., 2014. *Lab Chip* 14, 1087–1098.
- Parsa, H., Chin, C.D., Mongkolwisetwara, P., Lee, B.W., Wang, J.J., Sia, S.K., 2008. *Lab Chip* 8, 2062–2070.
- Porstmann, T., Kiessig, S.T., 1992. *J. Immunol. Methods* 150, 5–21.
- Reichert, J.M., 2001. *Nat. Biotechnol.* 19, 819.
- Ruslinga, J.F., Kumara, C.V., Gutkinde, J.S., Patel, V., 2010. *Analyst* 135, 2496–2511.
- Rissin, D.M., Kan, C.W., Campbell, T.G., Howes, S.C., Fournier, D.R., Song, L., Piech, T., Patel, P.P., Chang, L., Rivnak, A.J., Ferrell, E.P., Randall, J.D., Provuncher, G.K., Walt, D.R., Duffy, D.C., 2010. *Nat. Biotechnol.* 28, 595–599.
- Scallan, B., Cai, A., Solowski, N., Rosenberg, A., Song, X.Y., Shealy, D., Wagner, C.J., 2002. *Pharmacol. Exp. Ther.* 301, 418–426.
- Sharp, K.V., Adrian, R.J., 2004. *Exp. Fluids* 36, 741–747.
- Singhal, A., Haynes, C., Hansen, C.L., 2010. *Anal. Chem.* 82, 8671–8679.
- Song, M.Y., Park, S.K., Kim, C.S., Yoo, T.H., Kim, B., Kim, M.S., Kim, Y.S., Kwag, W.J., Lee, B.K., Baek, K., 2008. *Exp. Mol. Med.* 40, 35–42.
- Thaitrong, N., Charlermroj, R., Himananto, O., Seepiban, C., Karoonuthaisiri, N., 2013. *Plos One* 8, e83231.
- Wild, D., 2001. *The Immunoassay Handbook*. Nature Press, London.
- Wolf, M., Juncker, D., Michel, B., Hunziker, P., Delamarque, E., 2004. *Biosens. Bioelectron.* 19, 1193–1202.
- Yeh, F.L., Lin, W., Shen, H.D., Fang, R.H., 1997. *Burns* 23, 6–10.